# DESIGN OF POSITRON DAMPING RING FOR SUPER-KEKB

Mitsuo Kikuchi*, Tetsuo Abe, Kazumi Egawa, Hitoshi Fukuma, Kazuro Furukawa, Naoko Iida, Hitomi Ikeda, Takuya Kamitani, Ken-ichi Kanazawa, Kazuhito Ohmi, Katsunobu Oide, Kyo Shibata, Masafumi Tawada, Makoto Tobiyama, Demin Zhou, KEK, Tsukuba, Ibaraki, 305-0801 Japan

*Abstract*

Super-KEKB, an upgrade plan of the present KEKB collider, has recently changed its baseline-design from "high current" option to "nano-beam" scheme. The current is relatively low(4A/2.3A for LER/HER ring) compared to that of the high-current option(9.4A/4.1A), while the vertical beam size is squeezed to 60 nm at the interaction point to get the high luminosity. Since the Tousheck lifetime of LER is very short(600 sec), the intensity of the positron beam is as high as 8 nC/pulse. The emittance of the injected positron beam should be small enough to be accepted in the aperture of the LER. A damping ring has been proposed for the high-current option[1]. In this paper an updated design optimized to the nano-beam scheme is presented.

## INTRODUCTION

Super-KEKB, an upgrade plan of the KEKB collider, has recently changed its baseline-design from "high current" option to "nano-beam" scheme. The current is relatively low(4A/2.3A for LER/HER ring) compared to that of the high-current option(9.4A/4.1A), while the vertical beam size is 60 nm at the interaction point to get the high luminosity of $8 \times 10^{35}$ cm$^2$/sec . The vertical beta-function is squeezed to 0.27 mm at the IP. Narrow dynamic aperture, combined with very small beam volume in equilibrium, makes the beam lifetime very short, 600 sec, due to Tousheck effect. In order to maintain the beam current as well as to have rapid recovery from scratch, intensity of the injected positron beam has to be as much as 8 nC/bunch, assuming two bunches per Linac pulse with repetition frequency of 25 Hz. Positrons are generated at 4 GeV in the middle of Linac and subsequently captured and accelerated with L-band structures, yielding required charges with relatively high emittance and large energy spread. A damping ring(DR) is thus necessary to inject the positrons to the LER, which has very small acceptance in both of transverse and longitudinal planes. A schematics view of the system is shown in Fig. 1. The positron beam is subsequently accelerated to 1.1 GeV with S-band Linac before injected to the DR. A transport line from Linac to DR (LTR) is incorporated with a energy compression system(ECS) that rotates the longitudinal phase space to compress the energy spread within the energy acceptance of the DR. The bunch length of the extracted beam is compressed with the bunch compression system(BCS), which is embodied in the return line(RTL).

* mitsuo.kikuchi@kek.jp

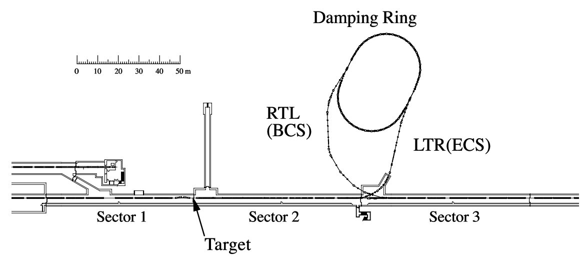


Figure 1: Layout of the system.

## PARAMETERS

Beam parameters of the incoming beam are shown in Table 1. Since the DR tunnel is rather shallow from the surface (2.3 m from surface to ceiling) radiation-safety regulations on the beam loss in the DR are expected to be stringent. The energy tail in the Linac being the most concern, energy collimators are placed in the first arc of the LTR, that truncate the tails and define a clear-cut energy bandwidth of the beam prior to injection to the DR[2]. The beam loss in the collimator depends on the compression ratio and amounts 10 % and 25 %, for the energy band-width of ±1.5 % and ±0.8 %, respectively[2]. These losses are acceptable owing to thick shields surrounding the collimators.

Table 1: Parameters of the injected beam

| | before ECS | after ECS | unit |
|---|---|---|---|
| Energy | 1.1 | | GeV |
| Repetition frequency | 50 | | Hz |
| Emittance | 1.7 | | $\mu$m |
| Energy spread† | 1.67 | 0.50 | % |
| Bunch length† | 2.67 | 11.7 | mm |
| Number of bunches | 2 | | |
| Bunch spacing | 98 | | ns |
| Bunch charge | 8 | | nC |

† defined as extension that contains 99.7% divided by 6.

Parameters of the DR are shown in Table 2. Assuming effective thickness of 4 mm for the injection septum of LER, the emittance of 12 nm is acceptable in the injection aperture of the LER. The emittance of extracted beam from DR has to be less than 44 nm, taking into account of acceleration from DR(1.1 GeV) to LER(4 GeV). Note that the injection aperture of LER is dominated by the septum width and less dependent on the beam emittance.

Table 2: Parameters of the Damping Ring

| | | | |
|---|---|---|---|
| Energy | 1.1 | | GeV |
| No. of bunch trains | 2 | | |
| No. of bunches / train | 2 | | |
| Circumference | 135.50207 | | m |
| Max. stored current | 70.8 | | mA |
| Energy loss / turn | 0.091 | | MV |
| Hor. damping time | 10.87 | | ms |
| Inj.-beam emittance | 1700 | | nm |
| Emittance (h/v) | 41.4 / 2.07 | | nm |
| Energy spread | $5.5\times10^{-4}$ | | |
| Coupling | 5 | | % |
| Extracted emittance (h/v) | 42.5 / 3.15 | | nm |
| Cavity voltage | 0.5 | 1.0 | MV |
| Bucket height | 0.81 | 1.24 | % |
| Synchrotron tune | 0.0152 | 0.0216 | |
| Bunch-length | 11.01 | 7.74 | mm |
| Phase advance/cell (h/v) | 64.39 / 64.64 | | deg |
| Momentum compaction | 0.0141 | | |
| Bend-angle ratio | 0.35 | | |
| No. of normal-cells | 40 | | |
| RF frequency | 509 | | MHz |
| Chamber diameter | 34 | | mm |

## OPTICS DESIGN

Since the inner diameter of the chamber, 34 mm, is relatively large it is difficult to design a bend having field greater than, say, 1.5 T. We have adopted special lattice, "Reverse-bend FODO", that enables short damping time using a relatively low field[1]. In the proposed lattice one of the bends in the ordinary FODO is reversed its bend direction while preserving the bend radius. Let $r$ a bend-angle ratio of the reversed bend to normal positive bend, a damping time is given by the following equation,

$$\begin{aligned} \tau &= \frac{3T_0}{r_e\gamma^3 J_x I_2} = \frac{3}{2\pi c\, r_e J_x}\frac{\rho}{\gamma^3}C\frac{1-r}{1+|r|} \\ &= \frac{3}{2\pi c\, r_e J_x}\frac{\rho}{\gamma^3}\left(2\pi\rho+\frac{1-r}{1+|r|}L_1\right) \qquad (1) \end{aligned}$$

where $L_1$ is a total length except bends and $C = 2\pi\rho(1+|r|)/(1-r)+L_1$ the circumference. One can see that the contribution of the length $L_1$ to the damping time is decreased by a factor $(1–r)/(1+|r|)$. Assuming bend radius of $\rho = 2.7$ m, $L_1 = 100$ m, and $r = 0.35$, the damping time gets shorter by 42 % comparaed to the normal FODO($r = -1$).

### *Dynamic Aperture*

Proposed ring has a sufficient dynamic aperture(DA). Simulation results for dynamic aperture is shown in Fig. 2. Tunes are ($\nu_x$,$\nu_y$)=(8.24, 7.265) and the assumed rf bucket height is 4 %. The red lines show the largest initial action of particles that survived 4000 turns, for each initial momentum deviation $\Delta p/p$. Thick (red) line is for the case of no machine errors, while thin (red) lines are for the case of machine errors with 20 random seeds. The errors are assumed to have Gaussian distribution with tails cut off at $3\sigma$: strength error of 0.1 %, and 0.2 % for quads and sexts, respectively, and random misalignments 0.15 mm, rotation 0.3 mrad for quads and sexts, and BPM offset of 0.15 mm. The (green) rectangle corresponds to the beam size of $3\sigma$and an energy width of $\pm1.5$ %.

However, if we add systematic multipole errors to the above machine errors, the DA dramatically decreases as shown in Fig. 2. In the simulation we have assumed systematic allowed-order multipoles, defined as the field deviation $\Delta B/B$ at a given radius (22 mm) as in Table 3. Field quality control at these levels is not easy but not impossible for the state-of-the-art magnet technology.

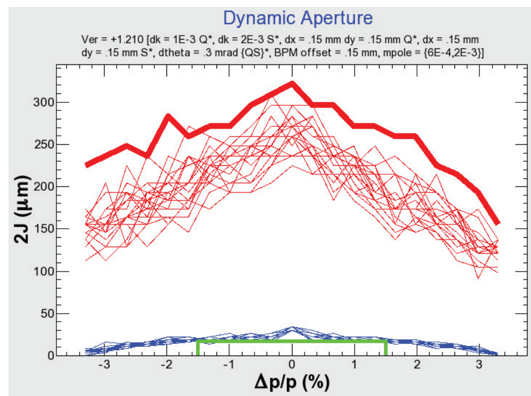


Figure 2: Dynamic aperture. Tunes are ($\nu_x$,$\nu_y$)=(8.24, 7.265). Thick (red) line is the DA in the case of an ideal machine, while thin (red) lines in the case of strength and misalignment errors(for details see text). Thin blue lines shows the case with above errors plus systematic high-order multipole errors.

Table 3: Systematic multipole errors

| Magnet | | | | $\Delta B/B$ |
|---|---|---|---|---|
| Bend | $K_2/K_0$ | 2.5 | $\mathrm{m}^{-2}$ | $6.0\times10^{-4}$ |
| | $K_4/K_0$ | $2.3\times10^{5}$ | $\mathrm{m}^{-4}$ | $2.3\times10^{-3}$ |
| Quad | $K_5/K_1$ | $3.1\times10^{5}$ | $\mathrm{m}^{-4}$ | $6.0\times10^{-4}$ |
| | $K_9/K_1$ | $1.5\times10^{16}$ | $\mathrm{m}^{-8}$ | $2.3\times10^{-3}$ |
| Sext | $K_8/K_2$ | $1.1\times10^{11}$ | $\mathrm{m}^{-6}$ | $6.0\times10^{-4}$ |
| | $K_{14}/K_2$ | $7.6\times10^{16}$ | $\mathrm{m}^{-12}$ | $2.3\times10^{-3}$ |

## BEAM INSTABILITIES

Beam instabilities are main concern in the design because the design bunch-charge is relatively high. In the course of design it was found that for shorter bunch-length (5 mm) and lower momentum compaction(0.006) an instability due to coherent synchrotron radiation(CSR) severely damages the beam performance and the instability threshold was lower than 1.6 nC. For the same parameters the electron cloud has also non-negligible effect.

### CSR induced Microwave Instability

Longitudinal wake potential per turn has been estimated for each component of vacuum duct, RF cavity, resistive wall, and CSR in which the rectangular cross section was assumed for the beam pipe. CSR as well as other component wake are shown in Fig. 3. CSR wake is tremendously large compared with other wakes. With this wake we have made multi-particle tracking simulation using two independent codes[3]. The results agree well and shown in Fig. 4 for four set of ring parameters, which are summarized in Table 4. We have also found that the instability is insensitive to the chamber diameter. The instability threshold seems well explained by Stupakov-Heifets 1-D theory[4] with free space CSR wake; For a perturbation wavelength $\lambda$, if the following inequality satisfies, the perturbed wave is unstable;

Table 4: Ring parameters for simulation

| | E(GeV) | $\alpha$ | $\sigma_z$(mm) | $\sigma_\delta$ | $\tau_\epsilon$(ms) |
|---|---|---|---|---|---|
| (a) | 1.0 | 0.0036 | 5.03 | $5.25\times10^{-4}$ | 6.3 |
| (b) | 1.1 | 0.0061 | 7.30 | $5.57\times10^{-4}$ | 6.9 |
| (c) | 1.1 | 0.0141 | 11.0 | $5.50\times10^{-4}$ | 5.4 |
| (d) | 1.1 | 0.0141 | 7.75 | $5.50\times10^{-4}$ | 5.4 |

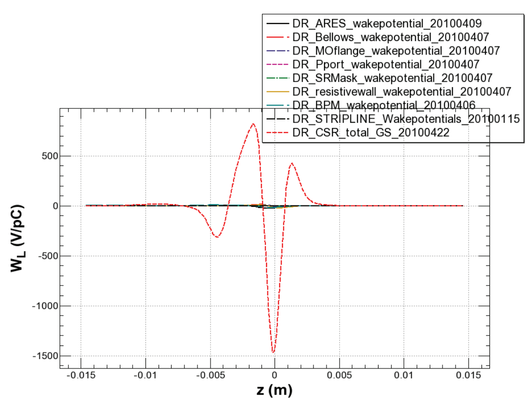


Figure 3: Longitudinal wake potential. (Red) broken line shows the CSR wake.

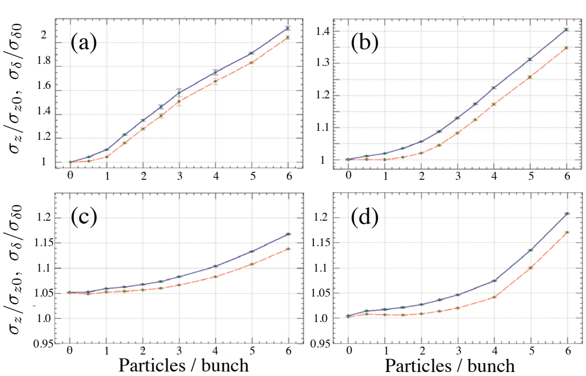


Figure 4: Energy spread and the bunch length as a function of the bunch intensity. The red(blue) line shows the energy spread(bunch length).

$$N_b > \frac{\pi^{1/6}}{\sqrt{2}} C \frac{1-r}{1+|r|} \frac{\gamma}{\rho^{1/3}} \alpha_p \sigma_\delta^2 \sigma_z \frac{1}{\lambda^{2/3}} \quad (2)$$

where $r$ is the bend ratio. If one take the wavelength $\min(\lambda_c, \sigma_z^{-1})$ as $\lambda$ for Eq. (2), $\lambda_c$ being the shielding threshold of beam pipe($\lambda_c = 2\sqrt{b^3/\rho}$), threshold is calculated as (a) $0.35\times10^{10}$ (b) $1.1\times10^{10}$ (c) $2.9\times10^{10}$ (d) $2.6\times10^{10}$ that are consistent with the tracking simulation results in Fig. 4

### Electron Cloud Instability

The threshold of electron density near the beam for the electron cloud instability(ECI) is given by[5]

$$\rho_{e,th} = \frac{2\ln 2\pi}{3\sqrt{2}} \frac{\gamma\nu_s\omega_e\sigma_z/c}{KQr_e\beta L}(1+\frac{\sigma_y}{\sigma_x}) \quad (3)$$

where, $\omega_e^2 = \lambda_+ r_e c^2/\sigma_y(\sigma_x+\sigma_y)$, Q=$\min(5, \omega_e\sigma_z/c)$, K=3, and L is the circumference. From Eq. (3) $\rho_{e,th} = 1.2\times10^{13}\,\mathrm{m}^{-3}$, $1.7\times10^{13}\,\mathrm{m}^{-3}$ for Vc=0.5 MV and 1.0 MV, respectively. We have made a tracking simulation for the same parameters, giving 40 % smaller threshold. Thus we define the threshold as $\rho_{e,th} = 0.52\times10^{13}\,\mathrm{m}^{-3}$. On the other hand we have made simulation study for the formation of the electron cloud in detail. The results are summarized in Table 5. SR is a photon-flux ratio to the design flux. Note that the electron density is not in proportional to the photon flux, which means that the electron density is saturated due to space charge effect. The integrated electron density $\rho L$ is $0.51\times10^{14}\,\mathrm{m}^{-2}$ for the case with $\delta_{\mathrm{max}} = 1$ and $SR = 1$. Comparing with the threshold of integrated electron density $\rho_{e,th}L = 7.0\times10^{14}\,\mathrm{m}^{-2}$, ECI seems not to be an issue for this parameter set, even taking uncertainty of electron cloud simulation into consideration.

Table 5: Electron density for various conditions

| Condition | Drift | Bend | Q+Sx | |
|---|---|---|---|---|
| $\delta_{\mathrm{max}} = 2$, SR=1 | 1.3 | 0.6 | 0.5 | $10^{12}\,\mathrm{m}^{-3}$ |
| $\delta_{\mathrm{max}} = 1$, SR=1 | 0.4 | 0.5 | 0.15 | $10^{12}\,\mathrm{m}^{-3}$ |
| $\delta_{\mathrm{max}} = 1$, SR=0.1 | 0.15 | 0.11 | 0.03 | $10^{12}\,\mathrm{m}^{-3}$ |

## REFERENCES

[1] M. Kikuchi, "Reverse-bend FODO lattice applied to damping ring for SuperKEKB", Nucl. Instr. Meth. A 556, pp.13-19 (2006)

[2] N. Iida, *et al.*, "Design of the Positron Transport System for SuperKEKB", this proceedings.

[3] For details see D. Zhou *et al.*, "CSR in the Super-KEKB Damping Ring", this proceedings.

[4] G. Stupakov and S. Heifets, "Beam Instability and Microbunching due to Coherent Synchrotron Radiation", Phys. Rev. Spec. Topics-Accel. and Beams, vol. 5, 054402(2002)

[5] K.Ohmi, KEK Preprint 2005-100.